Process Design, Development and Mechanical Analysis of Cu-Zn Alloy Produced by Sand Casting Process

Ilesanmi Afolabi Daniyan
Tshwane University of Technology
Adefemi Adeodu (femi2001ng@yahoo.com)
Department of Industrial & Mechanical Engineering, University of South Africa, Florida, 1709, South Africa
Oluwaseun Alo
Department of Mechanical Engineering, Vaal University of Technology, Vanderbijlpark, 1900, South Africa.
Bankole Oladapo
Coventry University Scarborough, YO11 2JW UK.

Research Article

Keywords: I-brass, casting, hardness, ultimate tensile strength, RSM

Posted Date: February 22nd, 2021

DOI: https://doi.org/10.21203/rs.3.rs-159895/v1

Process Design, Development and Mechanical Analysis of Cu-Zn Alloy Produced by Sand Casting Process

Ilesanmi Daniyan[1], Adefemi Adeodu[2], Oluwaseun Alo[3] Bankole Oladapo[4],

[1]*Department of Mechanical Engineering, Tshwane University of Technology, Pretoria 0001, South Africa.*
[2]*Department of Industrial & Mechanical Engineering, University of South Africa, Florida, 1709, South Africa.*
[3]*Department of Mechanical Engineering, Vaal University of Technology, Vanderbijlpark, 1900, South Africa.*
[4]*Coventry University Scarborough,* YO11 2JW *UK.*

Corresponding authors' email: afolabiilesanmi@yahoo.com Mobile: +27727021931

Abstract

In this study, the process design, development and mechanical analysis of Cu-Zn alloy produced by sand casting process were carried out. The process parameter optimization was carried out using the Response Surface Methodology (RSM) with the process conditions in the following range: temperature (300-500ºC) and zinc content (5-25%) having the hardness and ultimate tensile strength as the response of the designed experiment. The raw materials were scraps of copper wire and zinc battery casing and 13 different compositions of the alloy were prepared having the total mass for each weight percentage weighing 1.5 kg. The results obtained indicated that the hardness and ultimate tensile strength increases with an increases in the zinc content but decreases with an increase in the temperature. The elongation was however found to increase with an in increase in temperature but with a decrease in the zinc content. It is envisaged that the findings of this work will assist the brass material developers and the end users in the development of products with excellent mechanical properties.
Keywords: α-brass, casting, hardness, ultimate tensile strength, RSM

1. Introduction

The increasing quest for the materials with excellent properties capable of meeting the service and functional requirements has continued to trigger research interest in the field of materials development. The dynamic nature of technology, need for cost, energy and environmental sustainability as well as the changing products and industrial applications necessitate the development of materials with outstanding properties in order to meet these challenges. To a large extent, the quality of a product, cost effectiveness as well as its performance in service is a function of the materials employed for the development. Hence, the selection and the development of the right materials for the right application is a critical decision which affects the entire life cycle of a product from birth to the end of life. The motivation for this study stems from the quest to develop Cu-Zn alloy from scrap materials, thus, converting waste to wealth with improvement in the cost effectiveness of the final product. Cu-Zn alloy otherwise known as brass is a non-magnetic material which boast of good strength and ductility, high corrosion resistance, as well as good malleability and formability [1-4]. The alloy is made up of two principal materials namely copper and zinc in a varying proportion depending on the

intended application with other elements such as aluminum, phosphorus, manganese, silicon, and arsenic in small compositions [5-6]. Due to its excellent properties, Cu-Zn alloy find suitable applications in the automotive industry, electrical and electronics industries, decorative purposes, plumbing services, amongst others [7-10]. Furthermore, the quest for materials which can promote cost, energy and environmental sustainability are another attraction to the alloy. This is because significant high strength to weight ratio of the Cu-Zn alloy can be achieved through a carefully balanced composition of the parent materials and other alloying elements. The development of materials with significant high strength to weight ratio is critical in minimizing the energy consumed and improving the environmental friendliness during the products' life cycle. Furthermore, cost, energy and environmental sustainability via the development of materials which can be reclaimed into service via a suitable end of life option once the product reaches its end of life. Previous study have proven that Cu-Zn alloy has high affinity for the recycling process due to its non-ferromagnetic behaviour [11-12]. This makes its separation from ferrous metal easy and the recovered Cu-Zn alloy can be recycled through the process of melting, casting and extrusion. The ease of recycling will promote cost effectiveness, and the concept of circular economy which emphasizes tolerance for waste generation during the product's life cycle with improvement in the material, energy and environmental conservation. Previous studies have shown that preliminary process design with use of the Design of Experiment (DoE) technique via the use of Taguchi, Response Surface Methodology etc. can be employed for the determination of the feasible combinations of process parameters that will enhance excellent mechanical properties [13-16]. Previous studies have also shown that the microstructure and mechanical properties of brass can also be enhanced with a carefully balanced composition of Cu-Zn and other alloying elements, addition of additives as well as the use of appropriate heat treatment technique [17-18]. Many innovative approaches aimed at improving the microstructure and mechanical properties of brass alloy have been reported [19-21]. For instance, Imai *et al.* [22] reported that the strength of Cu-Zn alloy (brass alloy) can be improved via the addition of small amount of chromium in solid solution as the strength impact of Cr solid solution in Cu-Zn alloy was reportedly significant as opposed to brass alloy strengthening via Cr precipitation. Okayasu *et al.* [23] reported that copper alloy with improved mechanical properties such as high strength and ductility can be obtained by the addition of alloying elements in the following compositions: $Cu\text{-}Al_{9.3}\text{-}Fe_{3.8}\text{-}Ni_2\text{-}Mn_{0.8}$ or $Cu\text{-}Al_4\text{-}Zn_{25}\text{-}Fe_3\text{-}Mn_{3.8}$ produced via warm rolling at 473 K. Furthermore, Hsieh *et al.* [24] reported that the microstructure of brass alloy can be enhanced via the addition of Bi and Pb as alloying elements produced via the gravity casting method. Xiao *et al.* [25] identified the method of cryogenic dynamic plastic deformation as suitable for strengthening Cu-Zn alloy but with reduction in ductility due to the appearance of shear bands. On the other hand, Jha *et al.* [26] explained that the ductility can be enhanced via heat treatment involving the annealing of the brass alloys at a controlled temperature. Mapelli and Venturini [27] found that heat treatment via annealing at elevated temperature can sufficiently increase the ductility of the brass alloy but with reduction in the strength of the material. In addition, in terms of wear resistance and creep performance, Wu *et al.* [28] found that the presence of Cu in the brass alloy can secure the development of an alloy with excellent wear resistance and creep performance for a carefully balanced composition. Other approaches such as cryo-rolling and Spark Plasma Sintering have also been reported to impact the mechanical and microstructural

properties of Cu-Zn alloys [29-31]. However, there is still dearth of information regarding the combination of feasible process parameters that would promote excellent mechanical properties of brass alloy developed via the sand casting process. Hence, this is one of the focus of this work with the aim to establish a preliminary process design for the development of Cu-Zn alloy. In addition, the microstructural and mechanical properties of the developed samples evaluated will also assist manufacturers in the determination of the optimum range of process parameters. It is envisaged that the findings of this work will be beneficial to the brass materials developers and the industrial end users in the development of products with excellent mechanical properties whose life cycle will promote the concept of circular economy, as well as cost, energy, material and environmental sustainability. The succeeding sections present the materials and method employed in this study in order to achieve the set objectives as well as the discussion of the findings and the conclusion.

2. Materials and Method

The method used in the study is divided into two stages: numerical analysis and physical experimentation.

2.1 Numerical analysis

The design of experiment was carried out in order to optimize the process parameters. This was achieved using the Response Surface Methodology (RSM) and Central Composite Design (CCD).

2.1.1 *RSM and CCD design and analysis*

The design of experiment (DoE) was carried out using the Response Surface Methodology (RSM) and Central Composite Design (CCD). The RSM and CCD has the capability to identify the feasible combinations of process parameters and manufacturing conditions as well as their cross effects on the response of the designed experiment. In addition, the RSM can suitably study the interactive effects of the process parameters or conditions (independent variables) on the experimental response (dependent variables) [32-34]. For the purpose of this study, the annealing temperature and the percent content of the zinc were the two factors considered as the independent variables A and B respectively while the hardness and the tensile strength of the brass stand as the response (output) of the designed experiment. The RSM was further used for the correlation of the independent variables as a function of the dependent variables thus producing two mathematical models for the prediction of the hardness and the tensile strength of brass. The essence is to determine the optimum range of the process conditions that will bring about the development of material (brass) with excellent mechanical properties in addition to cost, energy, material and environmental sustainability. Using the design expert (version 8 software) the experimental design the Response Surface Methodology (RSM) and the Central Composite Design (CCD) produced 13 experimental matrices whose responses were determined via the physical experimentations.

The summary of the experimentation design involving two factors varied over three levels: the high level (+1), centre points (0) and low level (-1) leading to the production of 13 samples of brass are presented in Tables 1 and 2.

Table 1. Process conditions and their levels

Process conditions	Level-1	Level-2	Level-3
Temperature (°C)	300	400	500

Zinc content (%)	5	17.5	30

Table 2. Feasible combination of the process conditions

No of experiments/samples	Temperature (^oC)	Zn content (%)	Zn content (kg)	Cu content (kg)
1.	400.00	15.00	0.225	1.275
2	300.00	10.00	0.150	1.350
3	300.00	15.00	0.225	1.275
4	400.00	20.00	0.300	1.200
5	400.00	10.00	0.150	1.350
6	258.58	5.00	0.075	1.425
7	500.00	10.00	0.150	1.350
8	500.00	15.00	0.225	1.275
9	300.00	20.00	0.300	1.200
10	500.00	20.00	0.300	1.200
11	400.00	25.00	0.375	1.125
12	300.00	25.00	0.375	1.125
13	500.00	25.00	0.375	1.125

2.1.2 Analysis of Variance

The statistical analysis of the mathematical model produced via the RSM and CCD was carried out using Analysis of Variance (ANOVA). The ANOVA evaluates the statistical significance of the output of the model. A good model which validates the numerical experimentation is signalled by a "p-value Prob > F" which should be less than 0.050, a F-value greater than unity, a "Lack of Fit" which is statistically insignificant relative to the pure error, the predicted R square, R squared and the adjusted R Squared which should be within the same range and close to 1 as well as the adequate precision which measures the signal to noise ratio which should be greater than 4 [16].

2.2 The physical experimentation

The physical experimentation is divided into two main stages; sand cast production and sample characterization

2.2.1 Sand casting process

The choice of the sand casting process was informed by the fact Cu-Zn alloy has a relatively low melting temperature which makes the sand casting process quite feasible. The major raw materials were scraps of copper wire and zinc battery casing. Five (5) different compositions of the alloy were prepared as Cu – 5%Zn, Cu – 10%Zn, Cu – 15%Zn, Cu – 20%Zn and Cu – 30%Zn alloy respectively, with the total mass for each percentage composition weighs 1.5 kg according to Table 3. The sequence of the casting process involved pattern making, mould and core making, casting, demoulding, removal of runner and cast cleaning as presented in Figures 1a-d. Tensile test samples of specifications 75 mm × 100 mm × 350 mm were machined from the lather and the samples were heat treated in an OMSZON electrical furnace whose temperature varies from 250-500˚C via homogenization annealing in order to homogenize the composition. Next, the grinding and polishing operations of each test sample were carried out.

While the grinding operation removes the marks and irregularities on the surface of the specimen, the polishing operations cleans and smoothens the surface so as to obtain a more precise mechanical and microstructural (metallographic) analysis of the samples. The polishing operations were carried out using ECONET II polishing deck with emery cloth mounted on a rotating disc. Each of the samples was held against the alumina impregnated cloth while the wear debris were removed under a constant flow of water. Furthermore, the polished surfaces were etched with ferric chloride solution for 30 seconds, and subsequently dipped in concentrated nitric acid in order to remove any inherent stains. Using a magnification of ×400, a ACCUSCOPE metallographic microscope was used for the metallographic examination of the samples.

Table 3. Furnace Charge Calculation for Cu-Zn Alloys

Alloy	Copper (Kg)	Zinc (Kg)	Total Mass (Kg)
Cu - 5% Zn	1.425	0.075	1.5
Cu - 10% Zn	1.35	0.15	1.5
Cu - 15% Zn	1.275	0.225	1.5
Cu - 20% Zn	1.2	0.3	1.5
Cu - 30% Zn	1.125	0.375	1.5
Total	6.375	1.125	7.5

Figure 1. (a) Making of the sound mould (b) introducing the Cu/Zn into the crucible

(c) Pouring of the molten alloy (d) Cooling of the molten alloy in the sand

2.2.2 Hardness

The hardness of the cast brass alloy samples were examined using the Monsanto Hounsfield Tensometer with 1. 5 mm diameter indenter ball and 100 kg load in accordance to ASTM E 384 standard. The hardness of the material is the measure of the resistance offered by the material against indentation hence the depth of the impression by steel ball indenter. Each of the samples were placed on the hardness testing table and allowed to make contact with the steel ball indenter and the diameter of the indentation was measured using the microscope and micrometer. The Brinell's hardness number (BHN) was calculated according to Equation 1.

$$BHN = \frac{2P}{\pi D(D-\sqrt{(D^2-d^2)})} \quad (1)$$

Where: P is the applied load (kg), D is the diameter of the indenter (mm) and d is the diameter of indentation (mm).

2.2.3 Ultimate Tensile strength

The ultimate tensile strength is the maximum load the specimen can carry before rupture or plastic deformation. The ultimate tensile strength of the cast brass alloy samples were examined using the Monsanto universal tensile testing machine under the application of increasing stresses at varying strain rates and temperatures. The tensile tests were carried out according to the ASTM D638 standard. The measurements of the specimens in terms of the diameter and length etc. were taken and recorded and the specimen was loaded into the Hounsfield universal tensile testing machine where it was loaded to 75% of yield to ensure the specimen is fully seated in the jaws. The load was therefore released and the mercury indicator was set. The loads were recorded until the specimen breaks and the percent elongation of the specimen was measured. The tensile stress which represents the strength the material can withstand before yielding to failure and the corresponding strain (e) due to deformation from the load applied are expressed as Equations 2 and 3 respectively.

$$\sigma = \frac{P}{A} \quad (2)$$

$$e = \frac{l_f - l_o}{l_o} \quad (3)$$

Where;

P is the maximum load (kg) and A is the cross-sectional area of the material (mm^2), l_f is the final length (mm), l_o is the initial length (mm) and $l_f - l_o$ is the elongation. The area of the test pieces is the product of the nominal thickness and the width. Figure 2 presents the tensile strength specimen.

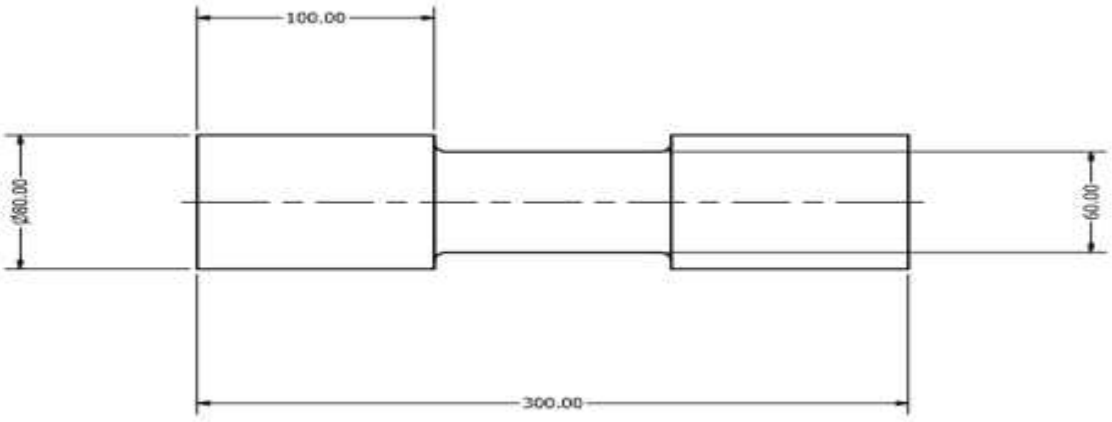

Figure 2. Tensile Strength Specimen

3. Results and Discussion

The experimental responses in terms of the hardness (BHN) and tensile strength using the combination of the process conditions given in Table 2 are presented in Table 4.

Table 4. Feasible combination of the process conditions

Temp. (°C)	Zn content (%)	Hardness (BHN)	Ultimate Tensile strength (MPa)	Tensile strength (MPa)	Original length (mm)	Final length (mm)	Strain	Elongation (mm)
400.00	10.00	30.3	355.6	296.33	30.00	34.08	0.136	4.08
400.00	15.00	53.9	360.9	300.75	30.00	33.72	0.124	3.72
300.00	10.00	85.6	380.8	317.33	30.00	33.99	0.133	3.99
300.00	15.00	45.7	378.9	315.75	30.00	32.88	0.096	2.88
400.00	20.00	51.9	369.9	308.25	30.00	33.00	0.10	3.00
258.58	5.00	56.8	370.6	308.83	30.00	30.66	0.022	0.66
500.00	10.00	26.3	286.3	238.58	30.00	34.77	0.159	4.77
500.00	15.00	20.8	302.75	252.29	30.00	34.09	0.136	4.09
300.00	20.00	77.5	379.7	316.41	30.00	32.50	0.083	2.5
500.00	20.00	23.7	318.6	265.50	30.00	33.99	0.133	3.99
400.00	25.00	44.5	370.5	308.75	30.00	32.85	0.095	2.85
300.00	25.00	50.1	410.6	342.16	30.00	32.27	0.075	2.27
500.00	25.00	24.5	334.4	278.66	30.00	33.97	0.132	3.97

3.1 Results from the numerical experimentation

The statistical analysis of the results obtained from both the numerical and physical experimentations presented in Table 5 used to obtain a predictive model which correlates the dependent variables (hardness and tensile strength) as a function of the independent process

parameters namely temperature and zinc content. The 2FI model equation obtained for the hardness and the quadratic model equation obtained for the tensile strength are presented in Equations 4 and 5.

$$Hardness = +46.23 - 16.07A + 7.18B - 17.17AB \quad (4)$$

Where; A is the temperature (^oC), B is the zinc content ($\%$).

$$Tensile\ strength = +360.44 - 38.75A + 27.80B + 7.02B + 16.62A^2 + 8.79B^2 \quad (5)$$

Where; A is the temperature (^oC), B is the zinc content ($\%$).

Table 5 presents the statistical analysis of the mathematical model obtained for harness prediction.

Table 5. The statistical analysis of the developed model (hardness)

Statistical parameters	Sum of Squares	df	Mean square	F value	p-value Prob > F	Remarks
Model	4605.53	3	1535.18	33.38	<0.0001	Significant
A-Temperature	1787.49	1	1787.49	38.87	0.0002	
B-Zinc content	184.16	1	184.16	4.00	0.0764	
AB	659.88	1	659.88	14.35	0.0043	
Residual	413.90	9	45.99			
Corr.	5019.43	12				

The model "F-value" (33.38) implies that the model is statistically significant, because there is only a 0.01% chance that the model "F-value" this large could occur due to noise. Furthermore, considering the value of the "p-value Prob > F" (<0.0001) which was significantly less than 0.050 indicates that the model terms are statistical significant. In this case, the significant model terms which can significantly influence the hardness of the cast brass alloy are A (temperature), B (zinc content), AB (the interactive effect of the temperature and the percent zinc content). The value of the correlation coefficients (R-Squared, Adjusted R-Squared Pred R-Squared) as well as the adequate precision are presented in Table 6. From Table 6, the values of R-Squared (0.9175), Adj R Squared (0.8901), Predicted R-Squared (0.8349) were within the same range and close to 1 which implies that the terms of the mathematical model are statistically significant. The closer the values to 1, the more significant the model terms and vice versa. In addition, the value of the adequate precision (17.294) which measures the signal to noise ratio is greater than 4, thus, indicating that the model significant for predictive purpose.

Table 6. The correlation coeffcients for the developed model

Parameter	Value	Remarks
R-Squared	0.9175	Significant
Adj R Squared	0.8901	Significant
Predicted R-Squared	0.8349	Significant
Adeq. Precision	17.294	Significant

Figure 3 is the normal plot of the residuals for the developed model for hardness. This plot indicates the extent to which the data set is normally distributed. The data set were observed to be close to the average diagonal line thus indicating that the residuals are approximately linear

although with inherent randomness left over within the error portion. The departure of data set points from the average diagonal line were minimal and found to be between the permissible range of ±10% in relation to the average diagonal line. The approximately linear pattern obtained is an indication of a normally distributed data set and the development of an accurate model which can be used for predictive and correlative purposes.

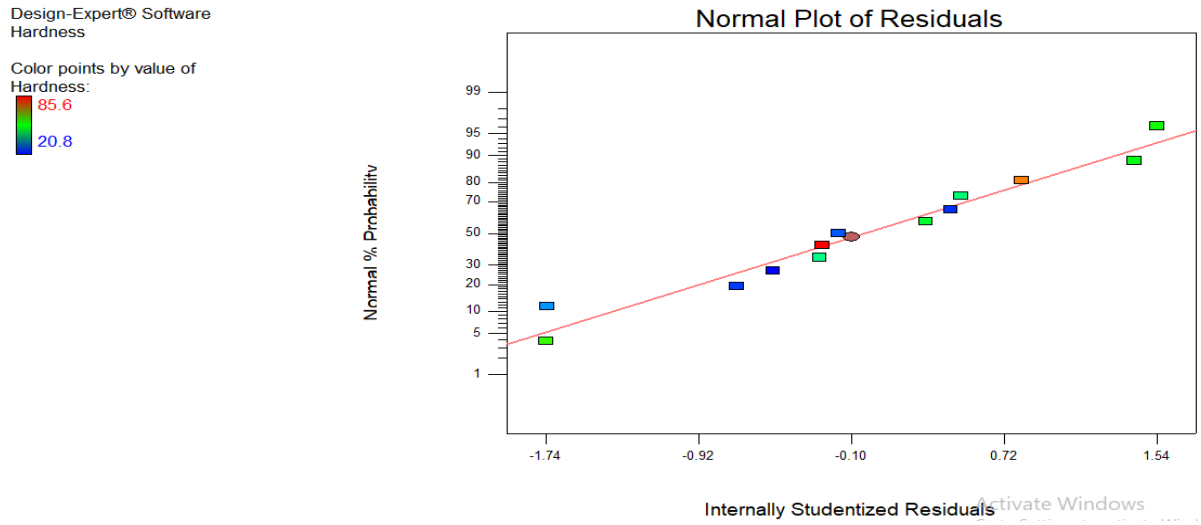

Figure 3. The normal plot of residuals (hardness)

Figures 4 and 5 present the contour and the interactive 3D plots of the effect of the temperature and zinc content on hardness. From the Figures there exist an inverse relationship between the zinc content and temperature as it affects the hardness of the developed samples. An increase in the percent zinc content leads to an increase in the hardness of the samples and vice versa. On the other hand, the hardness of the samples were observed to decrease with an increase in the temperature. As the zinc content increases from 5%-25%, the corresponding hardness were also observed to increase from 42.3228 MPa to 75.5636 MPa. On the contrary, an increase in temperature to 500°C reduces the magnitude of the hardness to 31.2424 MPa.

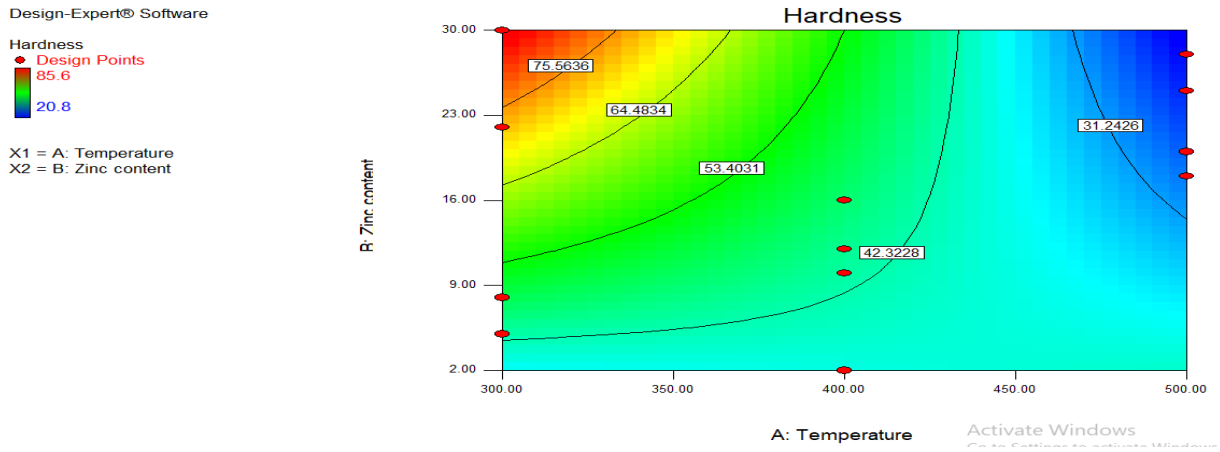

Figure 4. The contour plot of the effect of the temperature and zinc content on hardness

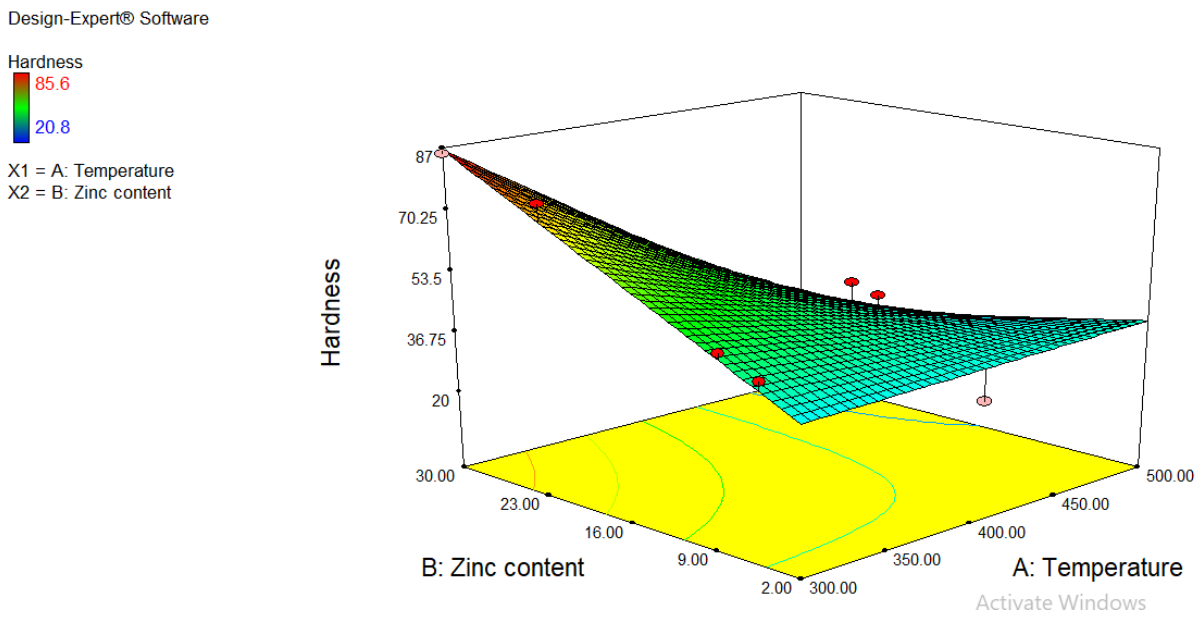

Figure 5. The 3D plot of the effect of the temperature and zinc content on hardness

Table 7 presents the statistical analysis of the mathematical model obtained for tensile strength prediction.

Table 7. The statistical analysis of the developed model (tensile strength)

Statistical parameters	Sum of Squares	df	Mean square	F value	p-value Prob > F	Remarks
Model	14404.58	5	2880.92	42.73	< 0.0001	Significant
A-Temperature	12504.90	1	12504.90	185.46	0.0001	
B-Zinc content	1482.94	1	1482.94	21.99	0.0022	
AB	80.38	1	80.38	1.19	0.3111	
A^2	833.00	1	833.00	12.35	0.0098	
B^2	23.67	1	23.67	0.35	0.5722	
Residual	471.99	7	67.43			
Corr.	14876.57	12				

The model "F-value" (43.73) implies that the model is statistically significant, because there is only a 0.01% chance that the model "F-value" this large could occur due to noise. Furthermore, considering the value of the "p-value Prob > F" (< 0.0001) which was significantly less than 0.050 indicates that the model terms are statistical significant. In this case, the significant model terms which can significantly influence the hardness of the cast brass alloy are A (temperature), A^2 (the square of the temperature), and B (the percent zinc content). The value of the correlation coefficients (R-Squared, Adjusted R-Squared Pred R-Squared) as well as the adequate precision are presented in Table 8. From Table 8, the values of R-Squared (0.9683), Adj R Squared (0.9456) and Pred. R-Squared (0.8984) were within the same range and close to 1 which implies that the terms of the mathematical model are statistically significant. The closer the values to 1, the more significant the model terms and vice versa. In addition, the value of the adequate precision (87.001) which measures the signal to noise ratio is greater than 4, thus, indicating that the model significant for predictive purpose.

Table 8. The correlation coeffcients for the developed model

Parameter	Value	Remarks
R-Squared	0.9683	Significant
Adj R Squared	0.9456	Significant
Pred. R-Squared	0.8984	Significant
Adeq. Precision	19.324	Significant

Figure 6 is the normal plot of the residuals for the developed model for the tensile strength. This plot indicates the extent to which the data set is normally distributed. The data set were observed to be close to the average diagonal line thus indicating that the residuals are approximately linear although with inherent randomness left over within the error portion. The departure of data set points from the average diagonal line were minimal and found to be between the permissible range in relation to the average diagonal line. The approximately linear pattern obtained is an indication of a normally distributed data set and the development of an accurate model which can be used for predictive and correlative purposes.

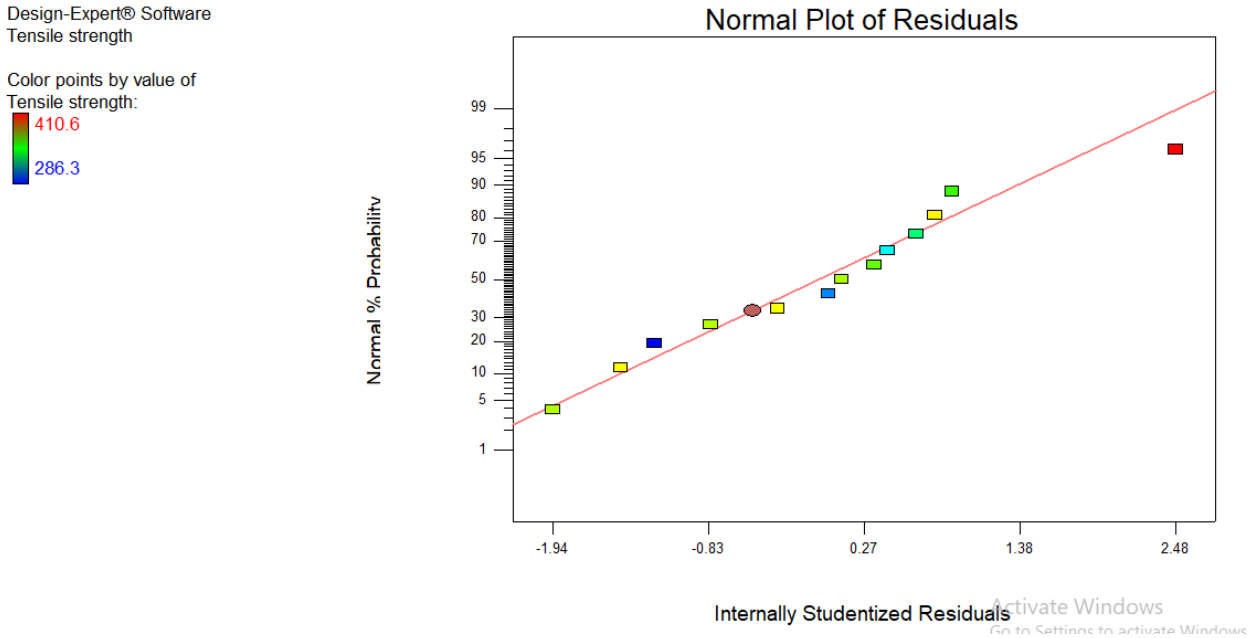

Figure 6. The normal plot of residuals (tensile strength)

Figures 7 and 8 present the contour and the interactive 3D plots of the effect of the temperature and zinc content on tensile strength. From the Figures there exist an inverse relationship between the zinc content and temperature as it affects the ultimate tensile strength of the developed samples. An increase in the percent zinc content leads to an increase in the ultimate tensile strength of the samples and vice versa. On the other hand, the ultimate tensile strength of the samples were observed to decrease from 360.758 MPa to 302.545 MPa with an increase in the temperature from 355^{o}C to 475^{o}C.

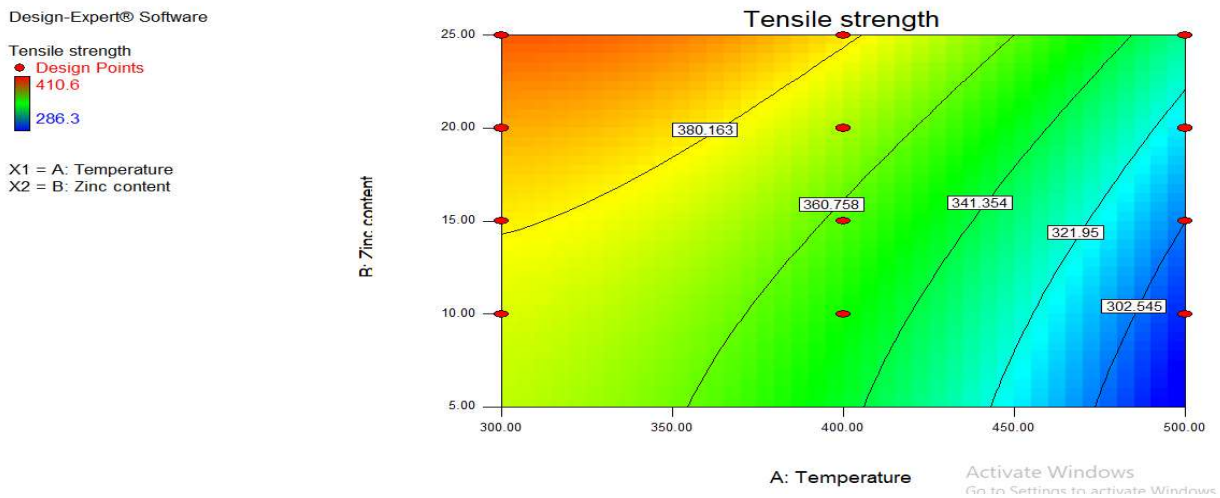

Figure 7. The contour plot of the effect of the temperature and zinc content on tensile strength

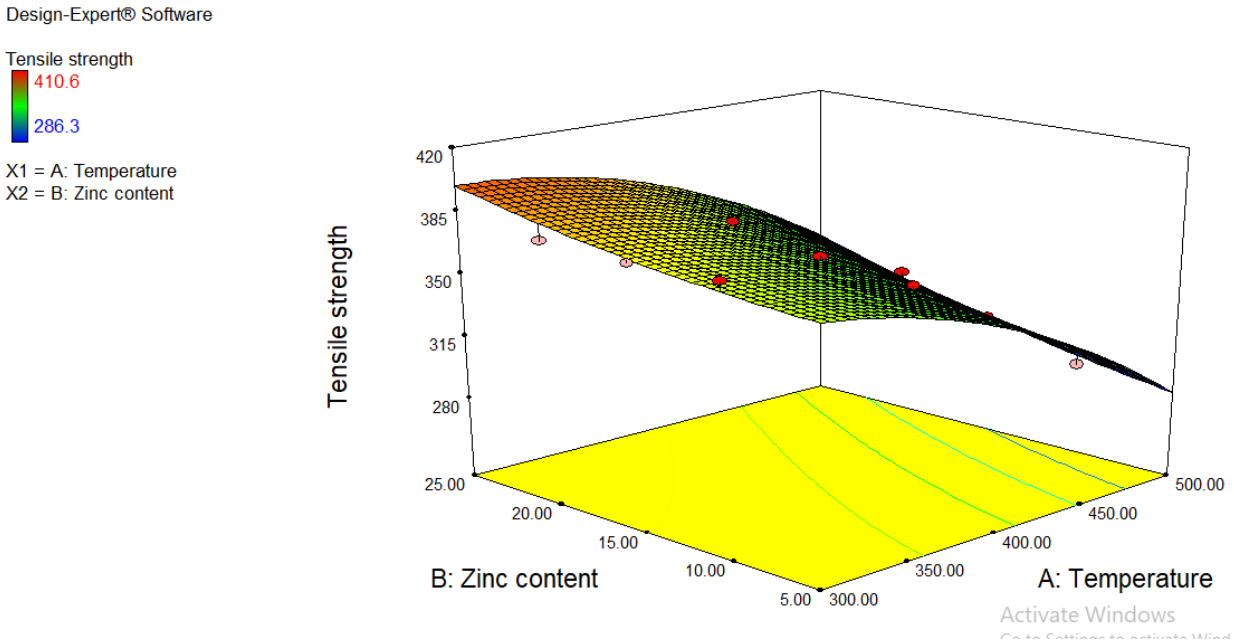

Figure 8. The 3D plot of the effect of the temperature and zinc content on tensile strength

Figure 9 presents the microstructural analysis of cast brass alloy samples at various process conditions. The colour of the developed samples were observed to change from red to golden brown with an increase in the percent zinc content.

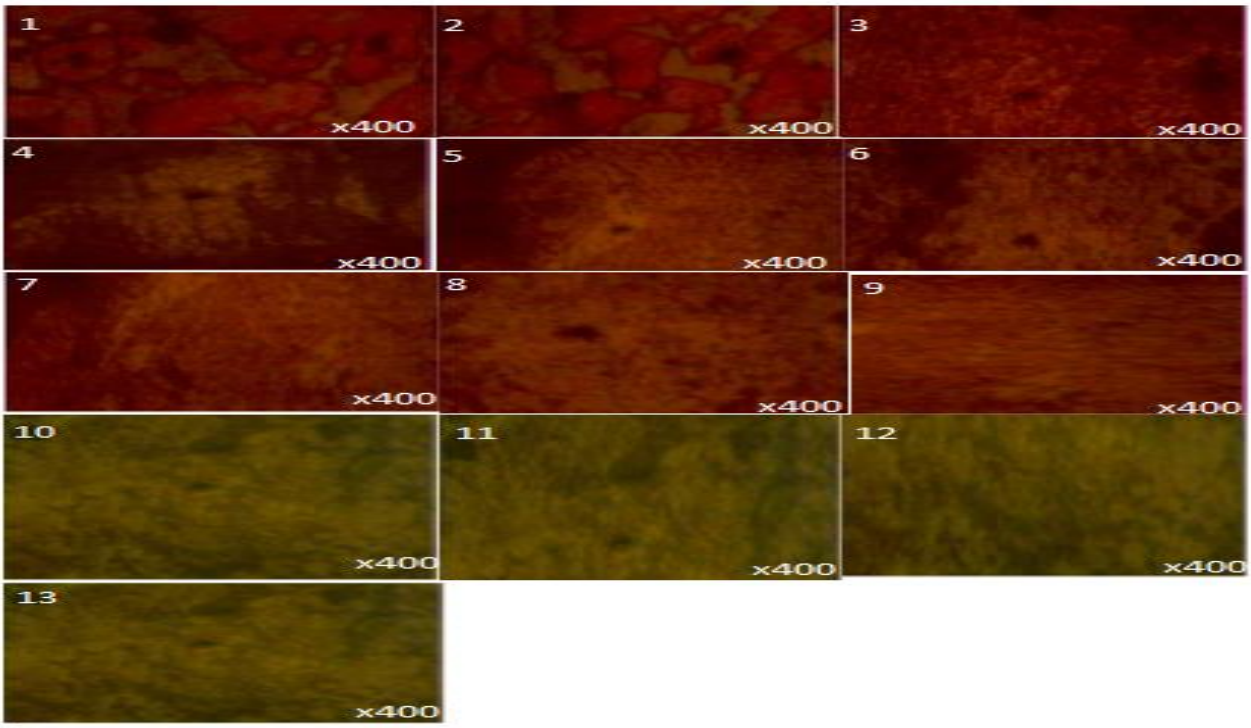

Figure 9. The microstructural analysis of cast brass alloy samples at various process conditions. **1.** 400 ºC, Zn-10%, **2.** 400 ºC, Zn-15%, **3.** 300 ºC, Zn-10%, **4.** 300 ºC, Zn-15% **5.** 400 ºC, Zn-20% **6.** 258.58 ºC, Zn-5% **7.** 500 ºC, Zn-10% **8.** 500 ºC, Zn-15% **9.** 300 ºC, Zn-20% **10.** 500 ºC, Zn-20% **11.** 400 ºC, Zn-25% **12.** 300 ºC, Zn-25% **13.** 500 ºC, Zn-25%

3.2 Effect of temperature variation on the ultimate tensile strength

The evaluation of the effect of temperature were carried out at 300ºC, 400 ºC, and 500ºC. From Figure 10, the ultimate tensile strength of the samples were observed to decrease with an increase in the temperature. This may be due to the fact that an increase in temperature above the recrytsllization temperature of the material often results in an increase in the grain size of the material thereby promoting the development of grain growth. The relationship between the tensile strength or hardness and grain size is inversely proportional. Large grain sizes brings about reduction in the tensile strength and hardness of the material and vice versa. The temperature increase promotes the dissolution of the brittle phase of the brass alloy as a result of homogenisation annealing with resulting increase in the ductility and toughness of the material. This is because the atom layers of the materials tend to break loose from the neighbouring bonds at increasing temperatures causing dislocation and free movement of the atoms thereby causing the reduction of internal residual stresses which improves the ductility and formability of the material but with reduction in the tensile strength and hardness [35].

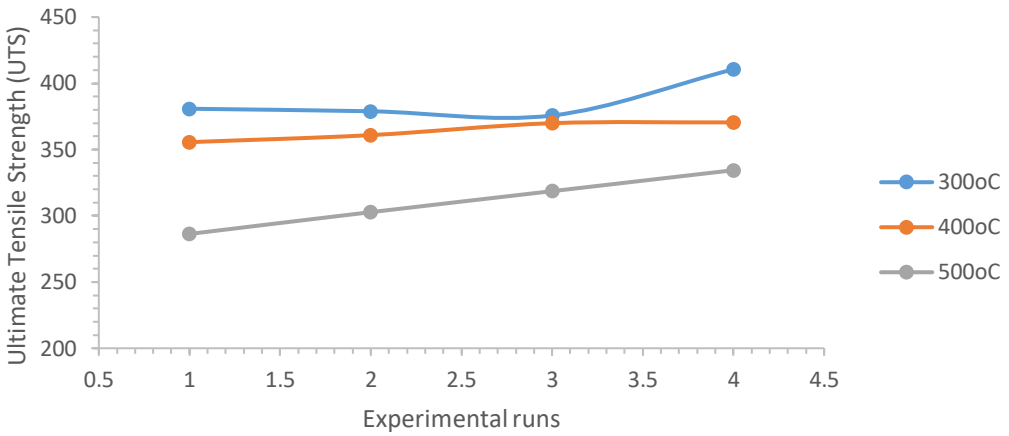

Figure 10. The ultimate tensile strength at varying temperature

3.2 Effect of temperature variation on hardness

The evaluation of the effect of temperature were carried out at 300ºC, 400ºC and 500ºC. From Figure 11, the hardness of the samples were observed to decrease with an increase in the temperature. This may be due to the fact that an increase in temperature activates dislocation motion which promotes easy migration of the atom from the neighbouring bonds [36].

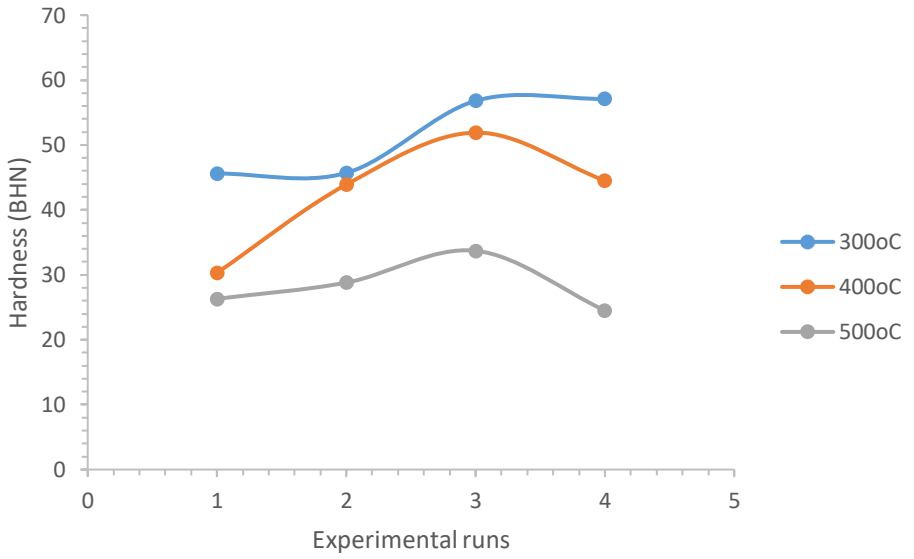

Figure 11. The hardness at varying temperature

3.3 Effect of zinc content variation on ultimate tensile strength

The evaluation of the effect of zinc content on the ultimate tensile strength of the samples were carried out at different zinc compositions: Zn-10%, Zn-15%., Zn-20%, Zn-25%. From Figure 12, the ultimate tensile strength of the samples were observed to increase with an increase in

the percent zinc content. An increase in the percent content of the zinc up to 35% promotes the dissolution of the composition of the constituents' materials to form a homogenized solid solution. Further increase in the zinc composition between 35%-45% will bring about phase transition from the alpha to the intermediate alpha-beta phase and subsequently beta phase [37]. The dissolution of the composition of the constituents' materials to form a homogenized solid solution via an increase in the percent zinc content results in the development of materials with smaller grain size. The smaller the grain size, the higher the tensile strength and hardness of the material and vice versa.

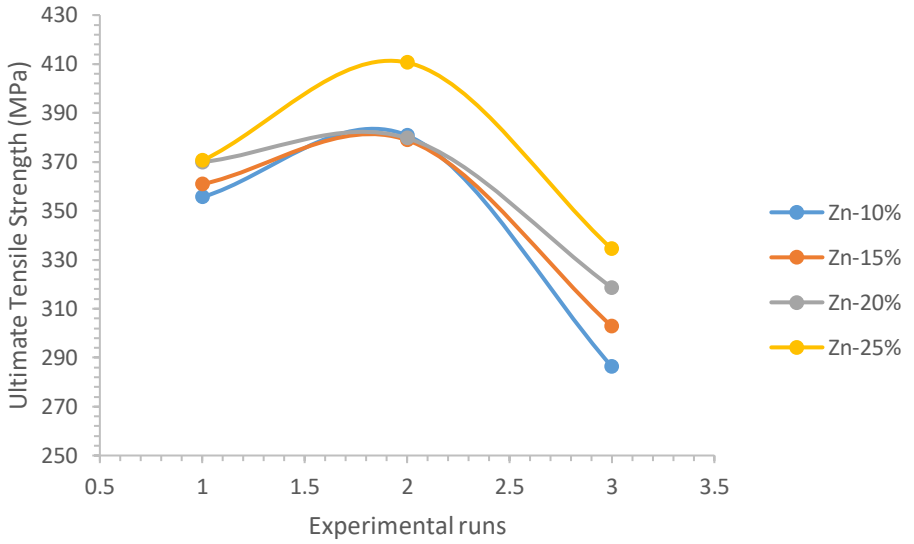

Figure 12. The ultimate tensile strength at varying zinc content

3.4 Effect of zinc content variation on hardness

The evaluation of the effect of zinc content on the hardness of the samples was carried out at different zinc compositions: Zn-10%, Zn-15%., Zn-20%, Zn-25%. From Figure 13, the hardness of the samples were observed to increase with an increase in the percent zinc content.

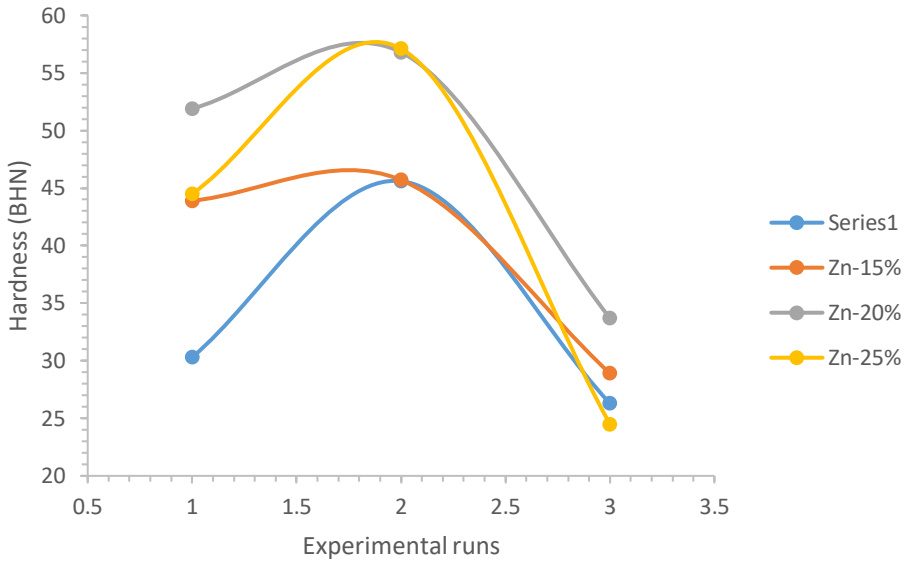

Figure 13. The hardness at varying zinc content

3.5 Effect of temperature variation on elongation

The evaluation of the effect of temperature were carried out at 300ºC, 400ºC and 500ºC. From Figure 14, the elongation of the samples were observed to increase with an increase in the temperature. This may be due to the fact that with an increase in temperature, the material deforms plastically thereby causing plastic flow with resulting increase in the elongation.

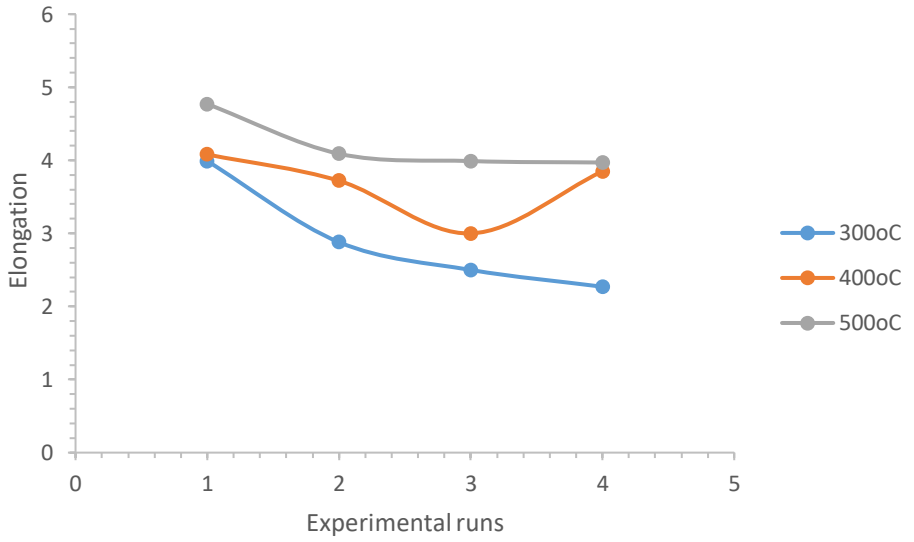

Figure 14. Elongation at varying temperature

3.6 Effect of zinc content variation on elongation

The evaluation of the effect of zinc content on the elongation of the samples were carried out at different zinc compositions: Zn-10%, Zn-15%., Zn-20%, Zn-25%. From Figure 15, the elongation of the samples were observed to decrease with an increase in the percent zinc content. The increase in the percent zinc content promotes increase in the localization of the

atoms of the constituents' material with resulting increase strength and reduction in the elongation. The results obtained for the elongation agree significantly with the findings of Lui *et al.* [38] on the investigation of the effects of annealing temperature and aluminum content on microstructures and properties of Al-brass.

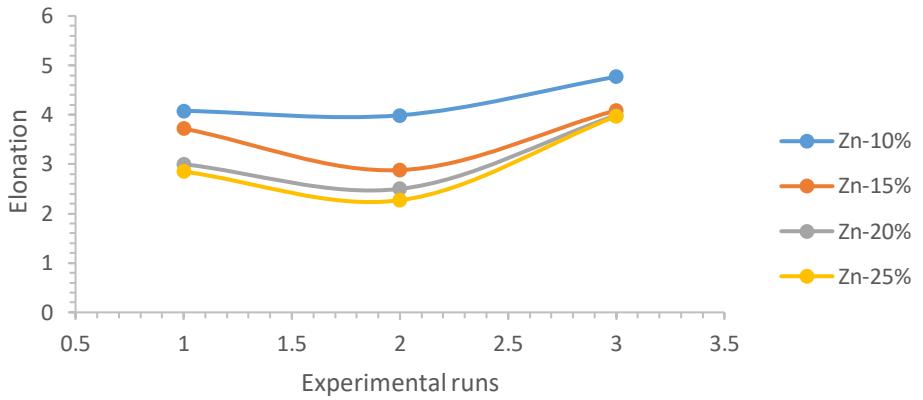

Figure 15. Elongation at varying zinc content

4. Conclusions

The process design, development and mechanical analysis of Cu-Zn alloy produced by sand casting process were carried out in this study. The results obtained indicated that the hardness and ultimate tensile strength increases with an increases in the percentage of the zinc content but decreases with an increase in the temperature. The elongation was however found to increase with an increase in increase in temperature but with a decrease in the percent zinc content. It is envisaged that the findings of this work will be beneficial to the brass materials developers and the industrial end users in the development of products with excellent mechanical properties whose life cycle will promote the concept of circular economy, as well as cost, energy, material and environmental sustainability.

DECLARATION

- Ethical Approval: The study requires no ethical approval.
- Consent to Participate: This is not applicable to this study.
- Consent to Publish: This is not applicable to this study.
- Authors Contributions: The conceptualization, experimentation, results analysis, writing-original draft, visualization, data curation, format analysis and editing were the collective work of the authors: Daniyan, I. A., Adeodu, A. O., Alo, A. O. & Oladapo, B. I.
- Funding: The authors disclosed receipt of the following financial support for the research: Technology Innovation Agency (TIA) South Africa, Gibela Rail Transport Consortium (GRTC), National Research Foundation (NRF grant 123575) and the Tshwane University of Technology (TUT)."
- Competing Interests: The authors declare no conflict of interest.
- Availability of data and materials: The data that support the findings of this study are openly available in public repository as listed in the references.

References

[1] Li, Y., Ngai, T.L., Xia, W. & Zhang, W. (1996). Effects of Mn content on the tribological behaviors of Zn-27% Al-2% Cu alloy. *Wear*, 198, 129–135.

[2] Gialanella, S. & Lutterotti L. Metastable structure in α-β brass. (2001). *J Alloys Comp.* 317–318:479–484.

[3] Zhu, Q., Wu, W., Liu, K., Chen, G., & Chen, W. (2009). Study on microstructure and properties of brass containing Sb and Mg. Science in China Series E: Technological Sciences. 52:2172-2174.

[4] Celdk, H., Aldirmaz, E. & Daksoy D. (2012). Effects of deformationon microstructure of Cu-Zn-Ni Alloy. *Gazi Univ J Sci*. 25(2):337–342.

[5] Hong, H. L Wang, Q., Dong, C. & Liaw P. K. (2014). Understanding the Cu-Zn brass alloys using a short-range-order cluster model: significance of specific compositions of industrial alloys. *Scientific Reports,* 4: 7065, pp. 1-4 | DOI: 10.1038/srep07065.

[6] Igelegbai, E. E., Alo, O. A., Adeodu, A. O. & Daniyan, I. A. (2017). Evaluation of mechanical and microstructural properties of *α*-Brass alloy produced from scrap copper and zinc metal through sand casting process. *Journal of Minerals and Materials Characterization and Engineering*, 5, 18-28.

[7] Karpagavalli R & Balasubramaniam R. (2007). Development of novel brasses to resist dezincification. *Corros Sci.* 49:963–979.

[8] Zhang, J., Wang, Q., Wang, Y. M., Li, C. Y., Wen, L. S. & Dong, C. (2010). Revelation of solid solubility limit Fe/Ni 5 1/12 in corrosion-resistant Cu–Ni alloys and relevant cluster model. *J. Mater. Res.* 25, 328–336.

[9] Çuvalcı, H. & Çelik, H. S. (2011). Investigation of the abrasive wear behaviour of ZA-27 alloy and CuSn10 bronze. *J. Mater. Sci.* 46, 4850–4857.

[10] Aldirmaz, E, Celik H, & Aksoy I. (2013). SEM and X-Ray diffraction studies on microstructures in Cu- 26.04%Zn-4.01Al alloy. *Acta Physica Polinica* A. 124:124–187.

[11] Imai, H., Kosaka, Y., Kojima, A., Li, S., Kondoh, K., Umeda, J. & Atsumi, H. (2010). Characteristics and machinability of lead-free P/M Cu60-Zn40 brass alloys dispersed with graphite, *Powder Technol.* 198:417-421.

[12] Maki, K., Ito, Y., Matsunaga, H. & Mori, H. (2013). Solid-solution copper alloys with high strength and high electrical conductivity, *Scr. Mater.* 68:777-780.

[13] Daramola, O. O., Tlhabadira, I. , Olajide, J. L., Daniyan, I. A., Sadiku, E. R. & Masu, L. (2019). Process design for optimal minimization of resultant cutting force during the machining of Ti-6Al-4V: response surface method and desirability function analysis. *Procedia CIRP* 84:854–860.

[14] Daniyan, I. A., Fameso, F., Ale, F., Bello, K. & Tlhabadira, I. (2020). Modelling, simulation and experimental validation of the milling operation of titanium alloy (Ti6Al4V). *The International Journal of Advanced Manufacturing Technology*, 109(7):1853-1866.

[15] Daniyan, I. A., Tlhabadira, I. Daramola, O. O., Phokobye, S. N., Siviwe, M. & Mpofu, K. (2020). Measurement and optimization of cutting forces during MS 200TS milling process using the Response Surface Methodology and dynamometer. *Procedia CIRP,* 88:288-293.

[16] Daniyan, I. A., Tlhabadira, I., Mpofu, K. and Adeodu, A. O. (2020). Development of Numerical Models for the Prediction of Temperature and Surface Roughness during the Machining Operation of Titanium Alloy (Ti6Al14V). *Acta Polytechnica Journal,* **60**(5):369–390, 2020.

[17] Hisashi, I., Shufeng, L., Atsumu, H., Kosaka, Y., Kojima, A., Umeda, J. & Kondoh, K. (2009). Mechanical properties and machinability of extruded Cu-40% Zn brass alloy with bismuth via powder metallurgy process. Transaction of JWRI, 38, 1-6.

[18] Ozgowicz, W., Kalinowska, E. O. & Grzegorczyk, B. (2010). The microstructure and mechanical properties of the alloy Cu-30% Zn after recrystallizion annealing. *Journal of Achievements in Materials and Manufacturing Engineering*, 40:1-10.

[19] Mamedov, A. & Mamedov, V. (2003). Microstructure, mechanical properties and tribological behaviour of PM Fe-Cu-Zn alloys containing solid lubricants. *Powder Metallurgy*, 46:311-8.

[20] Rollez, D., Pola, A.; Montesano, L., Brisitto, M.; De Felicis & D. Gelfi, M. (2017). Effect of aging on microstructure and mechanical properties of ZnAl15Cu1 alloy for wrought applications. *Int. J. Mater. Res.* 108:447–454.

[21] Dorantes-Rosales, H. J., López-Hirata, V. M., Hernández-Santiago, F., Saucedo-Muñoz, M. L. & Paniagua-Mercado, A. M. (2018). Effect of Ag addition to Zn22 mass%Al2 mass%Cu alloy on the four-phase reaction. *Mater. Trans.* 59:717–723.

[22] Imai, H. Li, S., Kondoh, K., Kosaka, Y., Okada, T., Yamamoto, K., Takahashi, M. & Umeda, J. (2014). Microstructure and mechanical properties of Cu40% Zn0.5% Cr alloy by powder metallurgy. *Materials Transactions*, 55(3): 528-533.

[23] Okayasu, M., Muranaga, T. & Endo, A. (2017). Analysis of microstructural effects on mechanical properties of copper alloys. *Journal of Science: Advanced Materials and Devices*, 2:128-139.

[24] Hsieh, C-C., Wang, J-S., Wu, P. T-Y. & Wu, W. (2013). Microstructural development of brass alloy with various Bi and Pb addition. *Met. Mater. Int.* 19 (6):1173-1179.

[25] Xiao, G. H., Tao, N. R. & Lu, K. (2009). Microstructures and mechanical properties of a Cu–Zn alloy subjected to cryogenic dynamic plastic deformation. *Materials Science and Engineering* A 513–514:13–21

[26] Jha, S. K., Balakumar, D. & Paluchamy, R. (2015). Experimental analysis of microstructure and mechanical properties of copper and brass based alloys. *International Journal of Automotive and Mechanical Engineering,* 11:2317-2331.

[27] Mapelli, C. & Venturini, R. (2006). Dependence of the mechanical properties of an a/b brass on the microstructural features induced by hot extrusion. *Scr Mater.*; 54:1169–1173.

[28] Wu, Z., Sandlöbes, S., Wang, Y., Gibson, J.S.K.-L. & Korte-Kerzel, S. (2018). Creep behaviour of eutectic Zn-Al-Cu-Mg alloys. *Mater. Sci. Eng.* A 724, 80–94.

[29] Sarma, V. S. Sivaprasad, K. Sturm, D. & Heilmaier, M. (2008). Microstructure and mechanical properties of ultrafine grained Cu-Zn and Cu-Al alloys produced by cryorolling and annealing, *Mater. Sci. Eng.* A 489:253-258.

[30] Wen, H., Topping, T. D., Isheim, D., Seidman, D. N. & Lavernia, E. J. (2013). Strengthening mechanisms in a high-strength bulk nanostructured Cu-Zn-Al alloy processed via cryomilling and spark plasma sintering, *Acta Mater.* 61:2769-2782.

[31] Daniyan, I. A., Tlhabadira, I., Phokobye, S. N., Mrausi, S., Mpofu, K. & Masu, L. (2020c). Modelling and optimization of the cutting parameters for the milling operation of titanium alloy (Ti6Al4V). 2020 IEEE 11th International Conference on Mechanical and Intelligent Manufacturing Technologies (ICMIMT 2020). Added to IEEE Xplore, pp. 68-73.

[32] Davoodi, B. & Tazehkandi, H. A. (2016). Cutting forces and surface roughness in wet machining of Inconel alloy 738 with coated carbide tool. Proceedings of the Institution of Mechanical Engineers, Part B: *Journal of Engineering Manufacture,* 230(2): 215-226.

[33] Khajelakzay, M. & S. R. Bakhshi (2017). Optimization of spark plasma sintering parameters of Si3N4-SiC composite using response surface methodology (RSM). *Ceramics International,* 43(9): 6815-6821.

[34] Daniyan, I. A., Tlhabadira, I., Phokobye, S. N., Siviwe, M. & Mpofu K. (2019). Modelling and optimization of the cutting forces during Ti6Al4V milling process using the Response Surface Methodology and dynamometer. *MM Science Journal*, 128:3353-3363.

[35] Kabash, Z. A. (2015). Effect of annealing on mechanical properties of brass alloy type C38500. *Diyala Journal of Engineering Sciences,* 8(1):16-25.

[36] Muhammed, A., Abed, A. & Mustafa, M. A. (2012). Effects of recrystallization temperature on the mechanical properties of CuZn30 alloy. The First National Conference for Engineering Sciences FNCES 2012, Baghdad, 2012, pp. 1-6. doi: 10.1109/NCES.2012.6740482.

[37] Sofyan, B. T. & Basori, I. (2016). Effects of deformation and annealing temperature on the microstructures and mechanical properties of cu-32% Zn brass. *ARPN Journal of Engineering and Applied Sciences,* 1(4):2741-2745.

[38] Liu, R., Shang, W., Huang, Z. & Wang, Y. (2012). Effects of annealing temperature and Al content on microstructures and properties of Al-brass. *Procedia Engineering,* 27:1823 – 1828.

Figures

Figure 1

(a) Making of the sound mould (b) introducing the Cu/Zn into the crucible (c) Pouring of the molten alloy (d) Cooling of the molten alloy in the sand

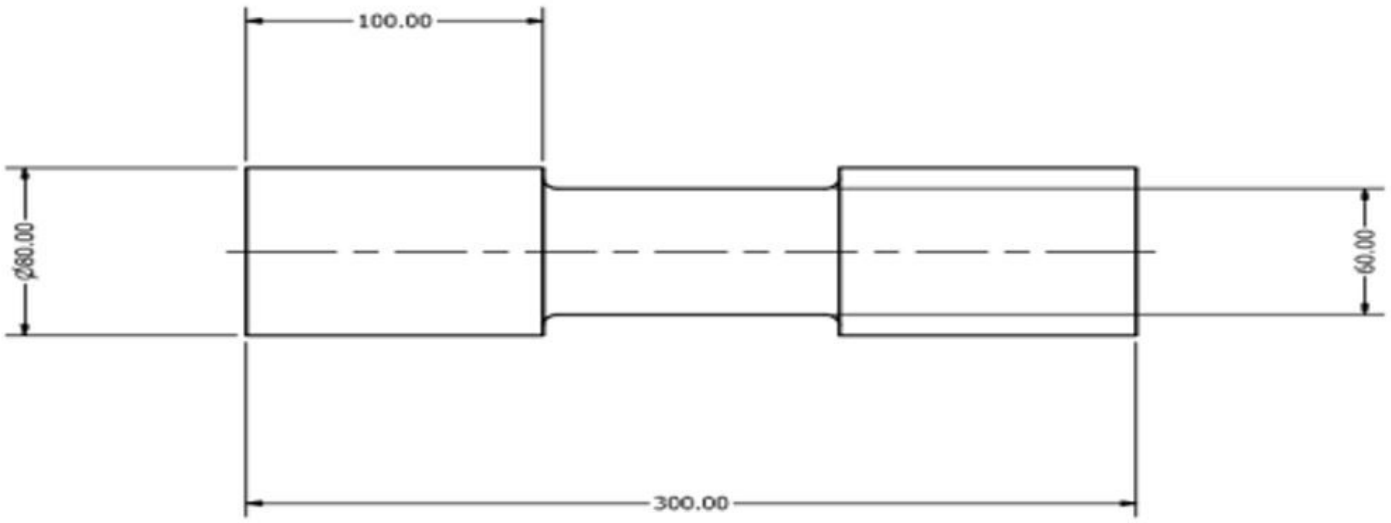

Figure 2

Tensile Strength Specimen

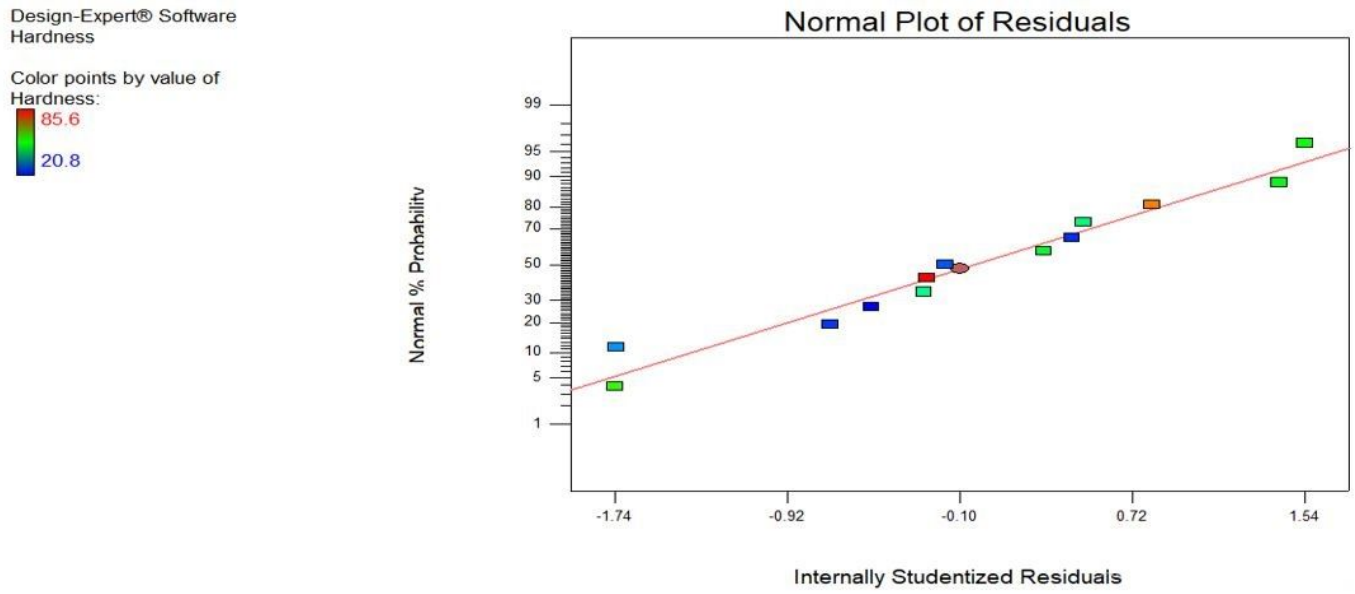

Figure 3

The normal plot of residuals (hardness)

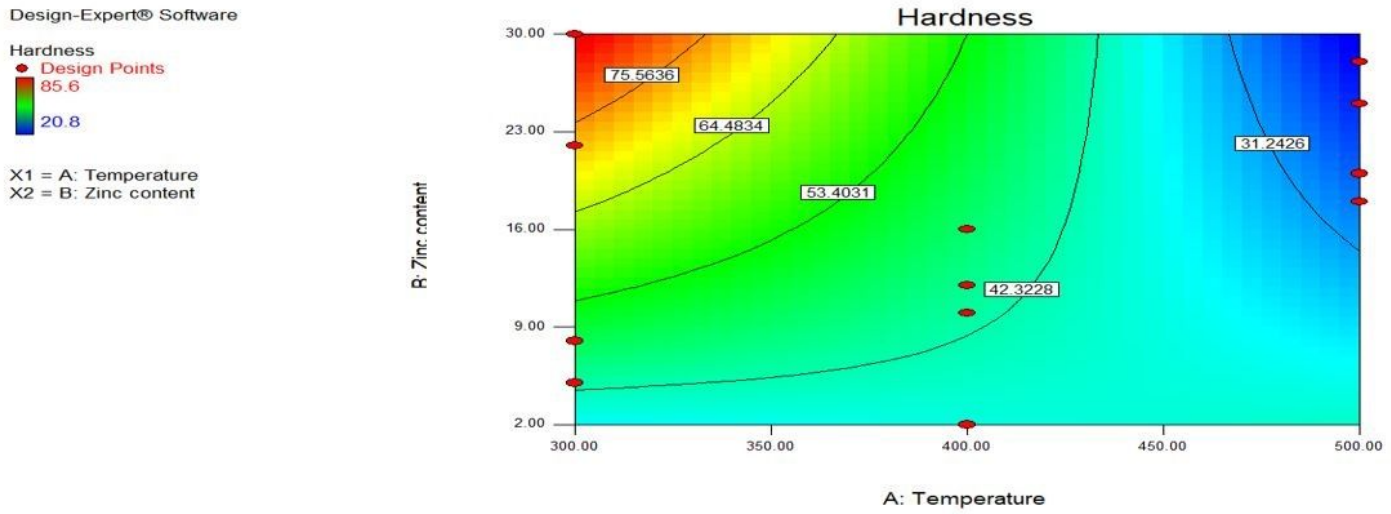

Figure 4

The contour plot of the effect of the temperature and zinc content on hardness

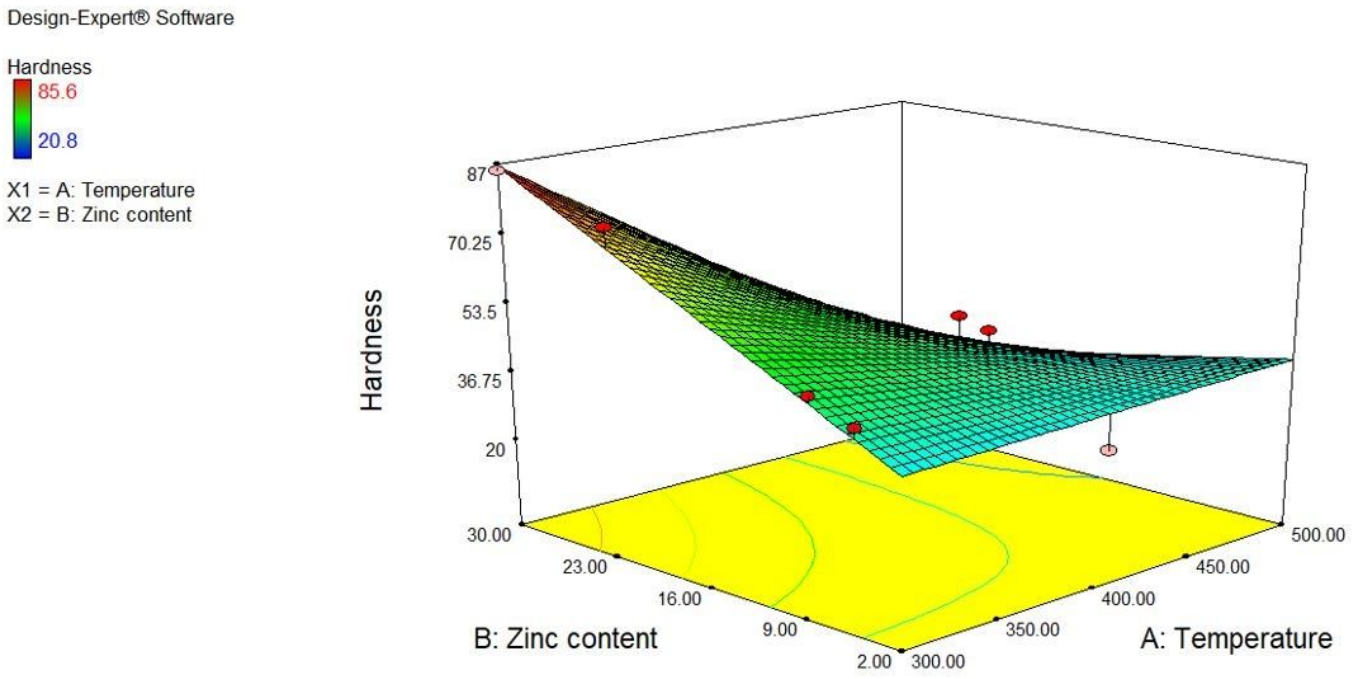

Figure 5

The 3D plot of the effect of the temperature and zinc content on hardness

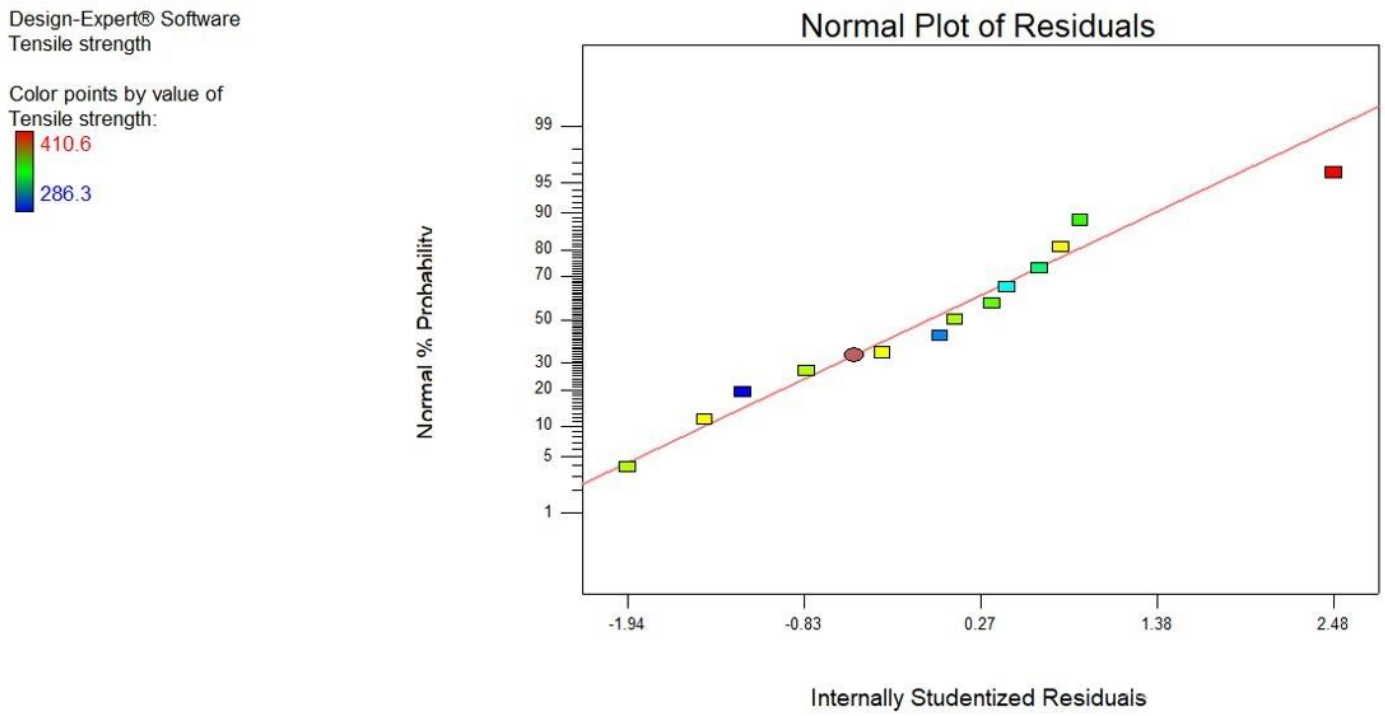

Figure 6

The normal plot of residuals (tensile strength)

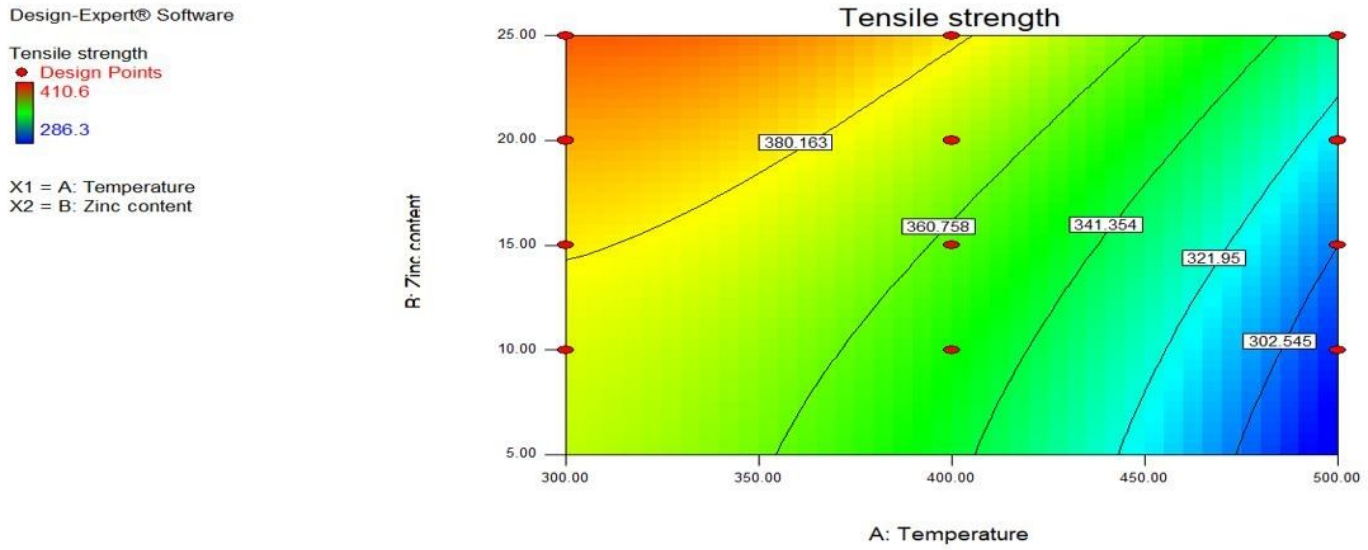

Figure 7

The contour plot of the effect of the temperature and zinc content on tensile strength

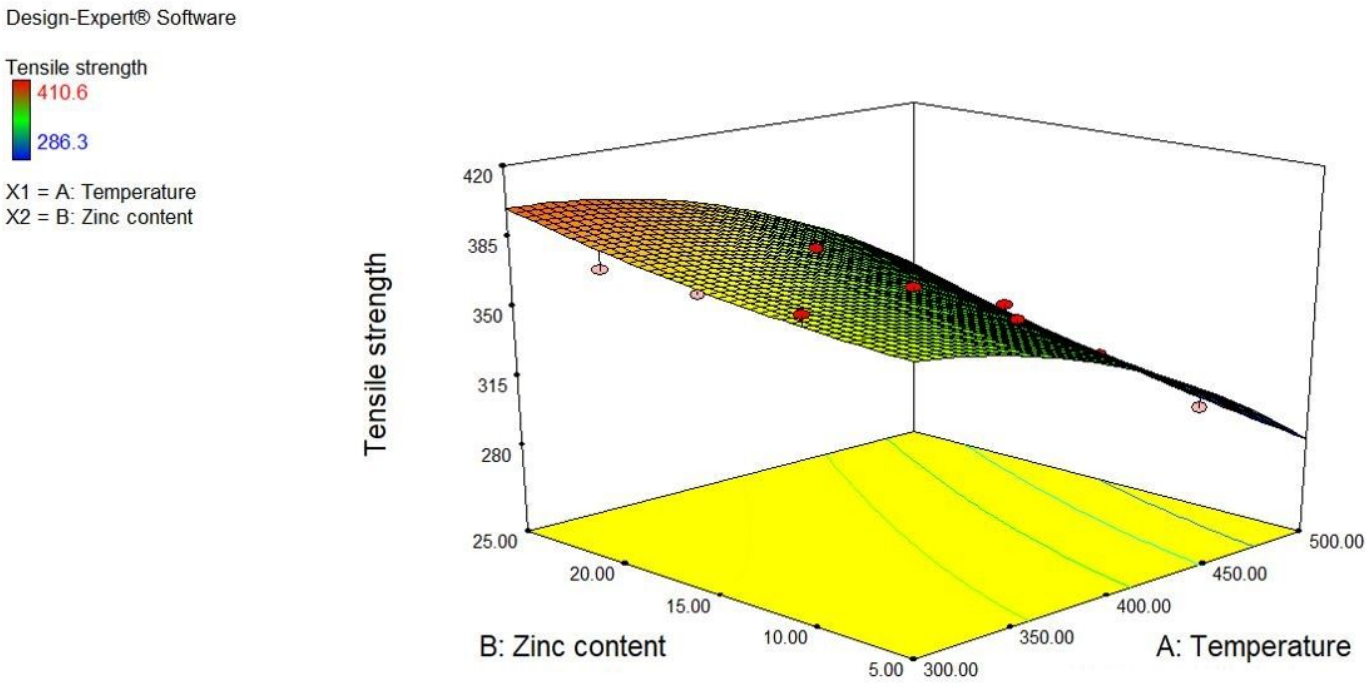

Figure 8

The 3D plot of the effect of the temperature and zinc content on tensile strength

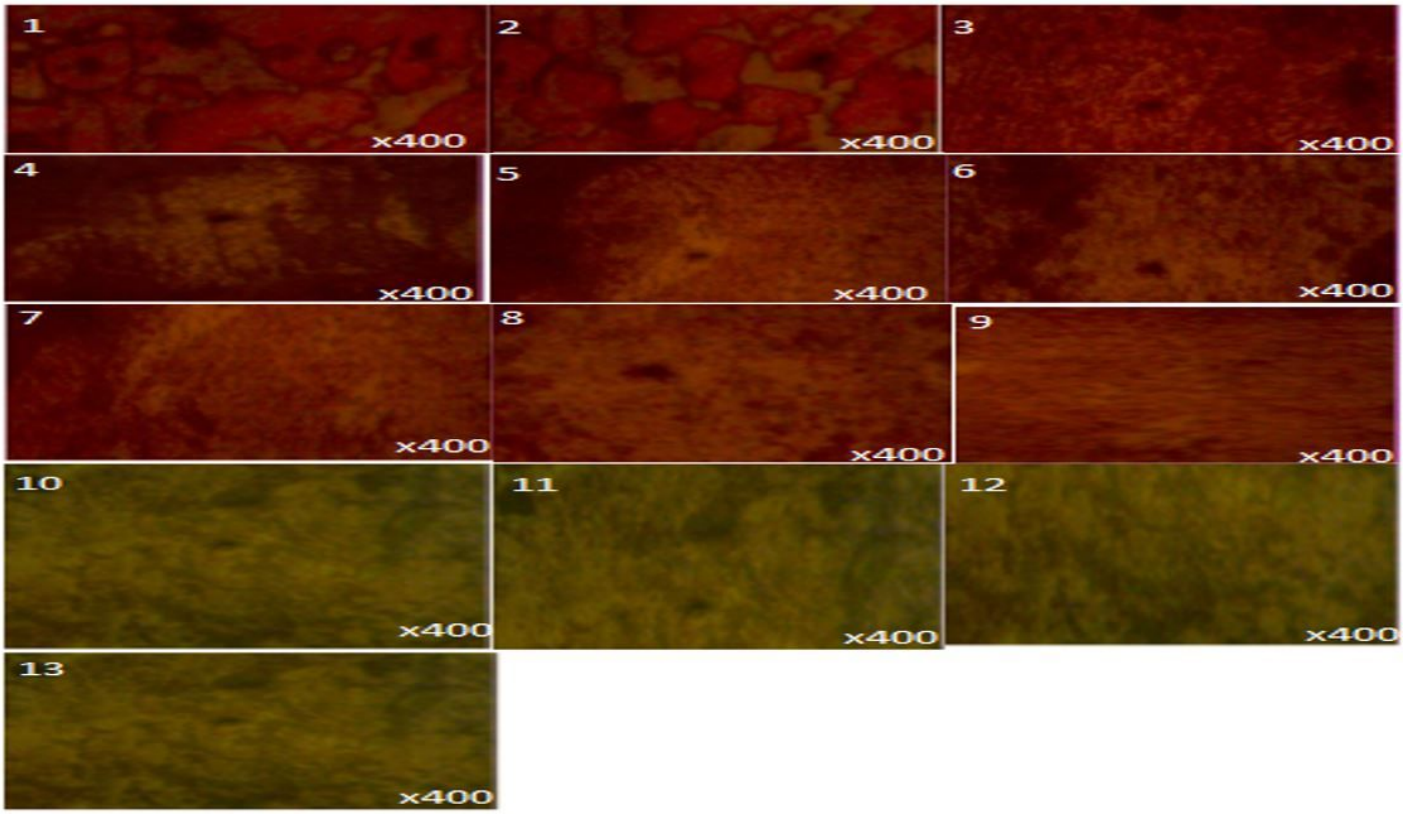

Figure 9

The microstructural analysis of cast brass alloy samples at various process conditions. 1. 400 oC, Zn-10%, 2. 400 oC, Zn-15%, 3. 300 oC, Zn-10%, 4. 300 oC, Zn-15% 5. 400 oC, Zn-20% 6. 258.58 oC, Zn-5% 7. 500 oC, Zn-10% 8. 500 oC, Zn-15% 9. 300 oC, Zn-20% 10. 500 oC, Zn-20% 11. 400 oC, Zn-25% 12. 300 oC, Zn-25% 13. 500 oC, Zn-25%

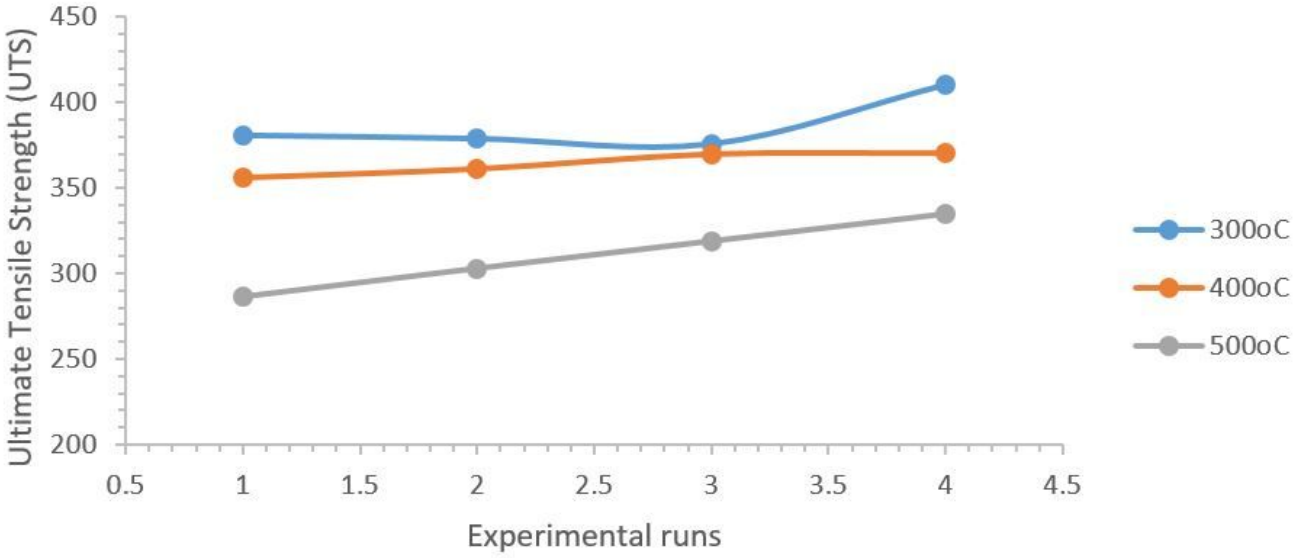

Figure 10

The ultimate tensile strength at varying temperature

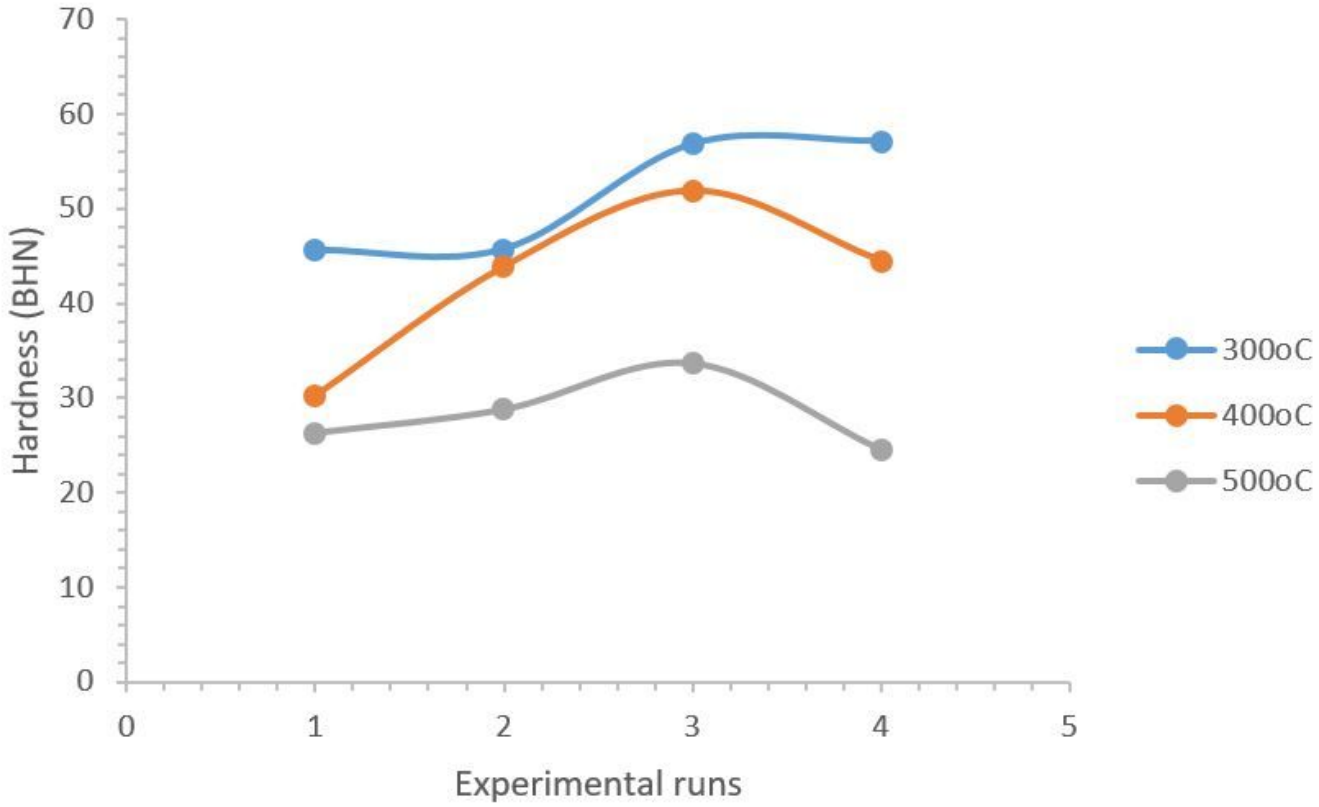

Figure 11

The hardness at varying temperature

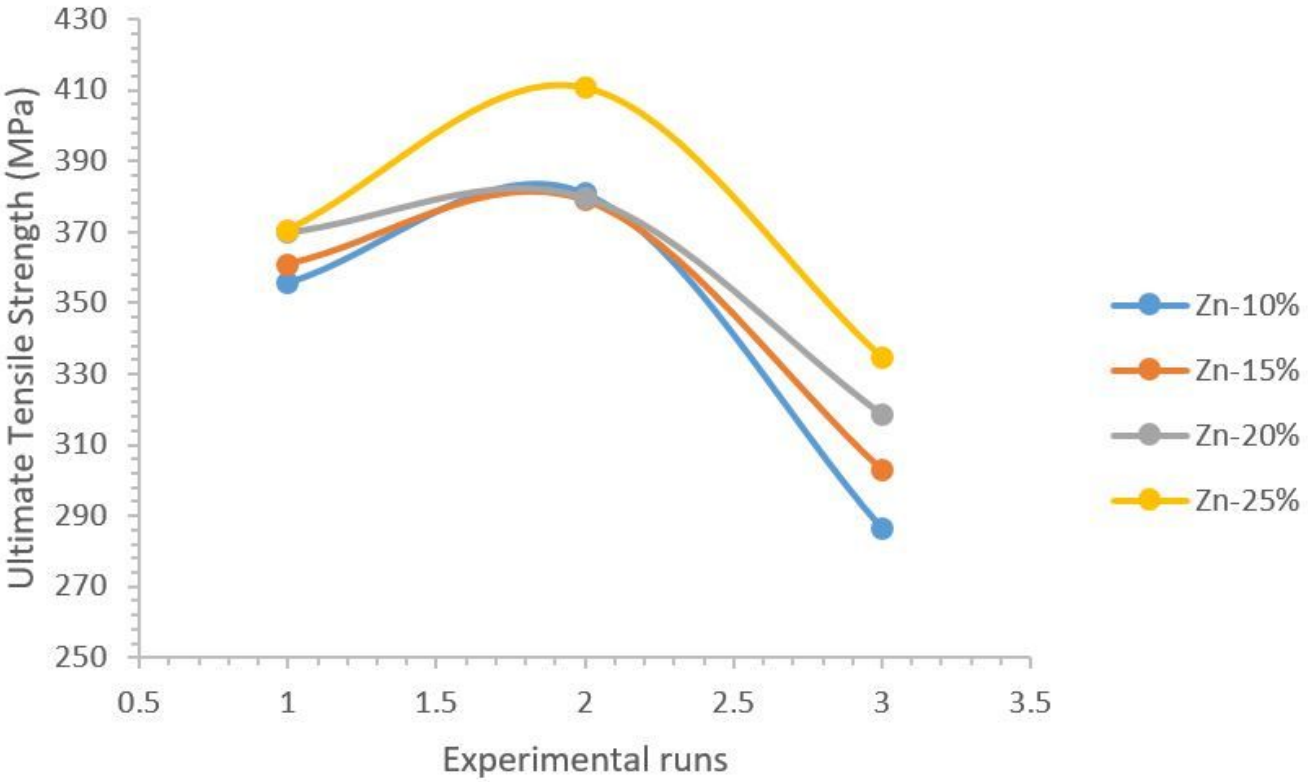

Figure 12

The ultimate tensile strength at varying zinc content

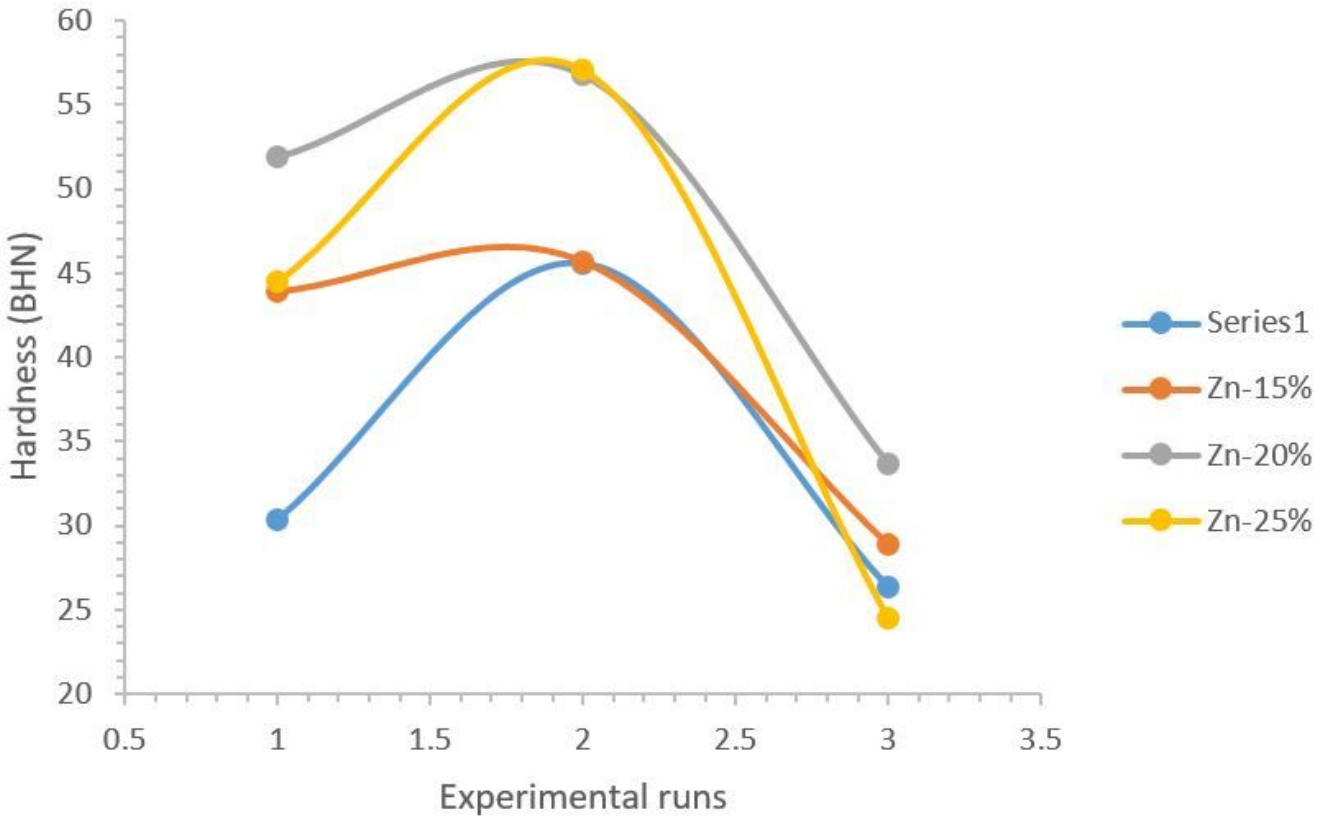

Figure 13

The hardness at varying zinc content

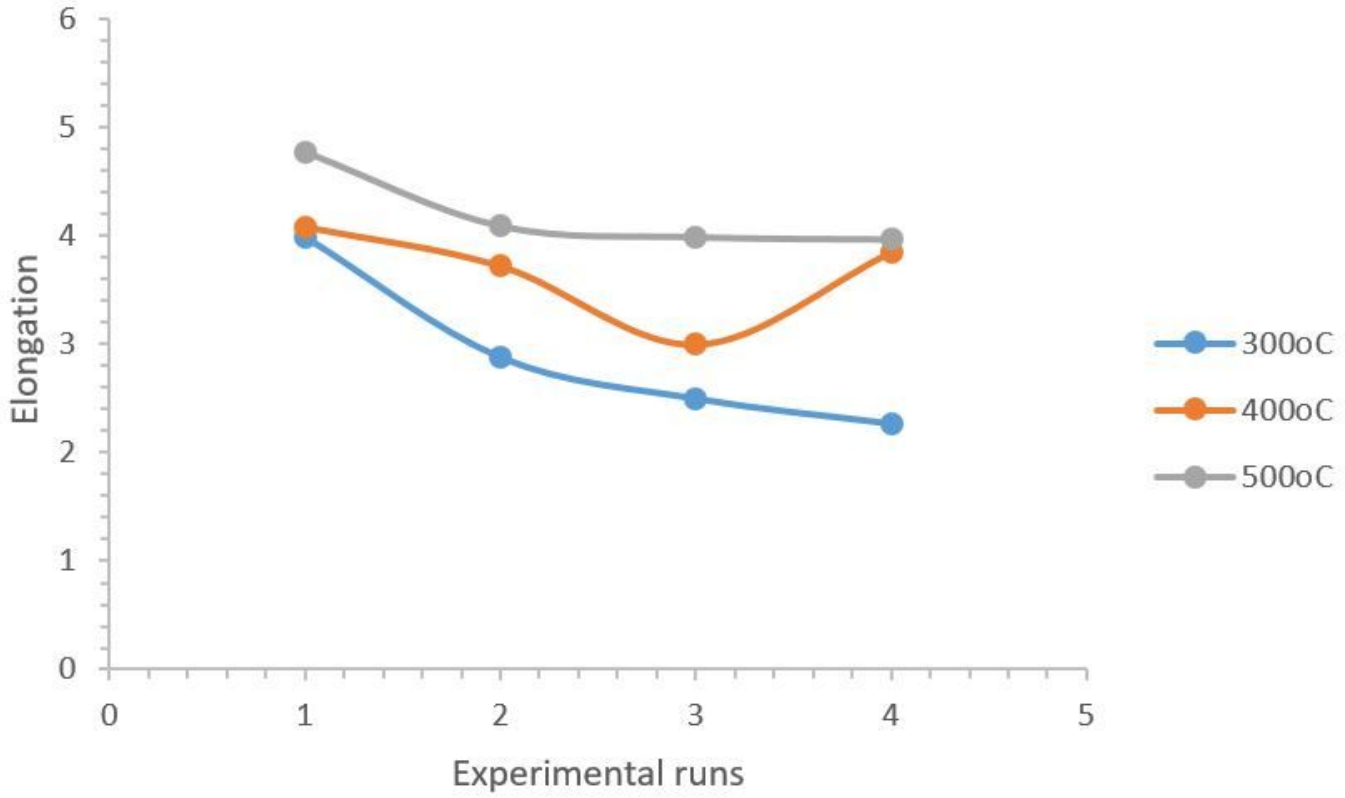

Figure 14

Elongation at varying temperature

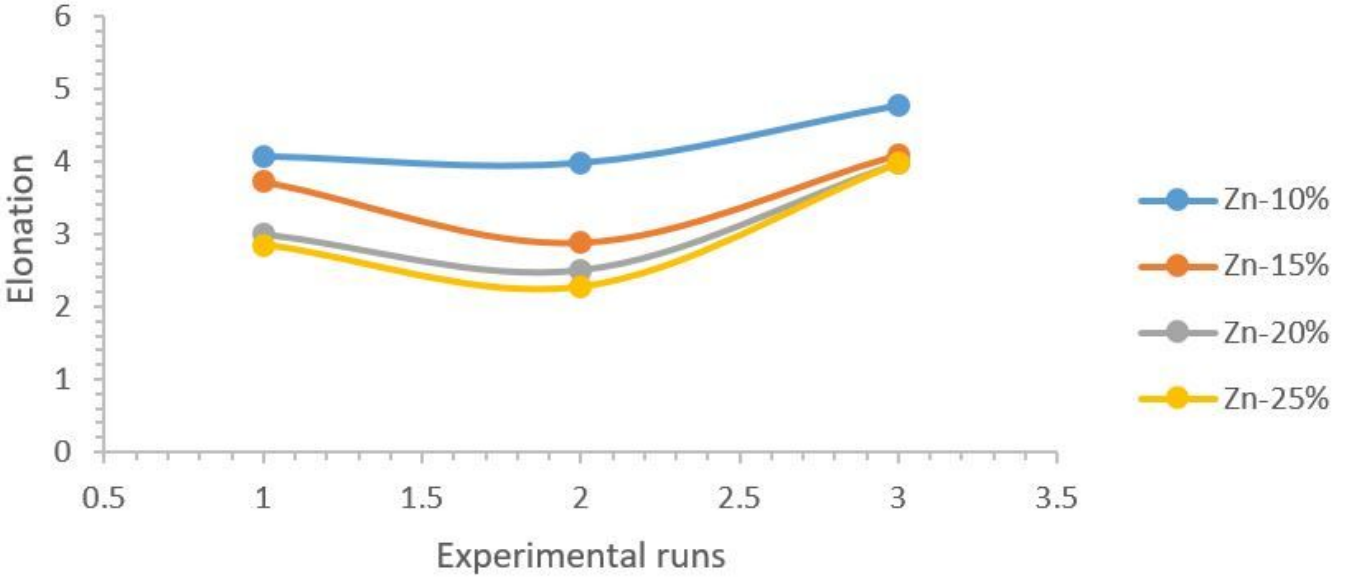

Figure 15

Elongation at varying zinc content